CHEMISTRY
A EUROPEAN JOURNAL

DOI: 10.1002/chem.201000068

Facile Electrochemical Preparation of Ag Nanothorns and Their Growth Mechanism

Yi-Min Fang,[a] Zhi-Bin Lin,[a] Yong-Ming Zeng,[a] Wen-Kai Chen,[a] Guo-Nan Chen,[a] Jian-Jun Sun,*[a] Bin Ren,*[b] and Zhong-Qun Tian[b]

Metal nanoparticles have attracted great interest owing to their important applications in catalysis, electronics, photonics, sensing, and information storage.[1,2] Numerous efforts have been devoted to controlling the shape, size, and composition of nanoparticles because the physical and chemical properties of nanocrystals critically depend on the these factors.[3,4] To date, a lot of metal nanoparticles with different shapes have been reported,[1] for example, the perfect/truncated cube[5] and tetrahedron,[6] triangular/hexagonal plate,[7,8] rectangular rod,[9] and right bipyramid.[10] It has been found that the catalytic activity of Pt nanoparticles is shape dependent.[11] The thermal switching behavior of nanoscale Fe islands are strongly affected by the particle shape.[12]

Ag and Au nanoparticles are of particular interest because both of them show a wide range of color owing to the localized surface plasmon resonance (LSPR). Surface enhanced Raman spectroscopy (SERS) can use the LSPR to enhance the species in direct contact with, or in the vicinity of, the surface. SERS has now been widely used for monitoring the surface species on electrode surfaces for mechanistic studies[13] and for ultrasenstive analysis[14,15] such as single molecule and single nanoparticle detection.[16] Nanoparticles of Ag and Au or their alloys have been used in these studies. Theoretical investigation has revealed that metal nanoparticles with a very large aspect ratio or sharp tips are likely to exhibit higher SERS activity over normal nanoparticles owing to the additional lightning-rod effect of the sharp tip to the LSPR of the nanoparticles.[17,18] Because Ag shows the best SERS activity compared with other substrates,[9] synthesis of Ag with sharp tips would be highly desirable. However, reports on preparing nanoparticles with sharp tips are relatively rare.[19]

On the other hand, electrochemical methods can be used as electrochemical controls such as potential, current, or charge, on the reaction processes such as deposition and dissolution. Electrochemical methods have the advantages of high flexibility, rapidity, ease of control, adoptability, and low-cost compared with wet-chemical approaches.[20] This method has, therefore, been used as a facile method for preparation of metal nanoparticles. For example, Sun and co-workers[21,22] combined chemical and electrochemcial methods and successfully obtained Pt and Pd nanoparticles with a high-index exposed plane such as the tetrahexahedral Pt nanocrystals, trapezohedral and concave hexoctahedral Pd nanocrystals, and Pt nanorods, which are not readily achievable by wet-chemical synthesis methods. Herein, we report the synthesis of Ag nanoparticles with sharp tips and a well-defined Ag (111) surface in only approximately 1–2 min by simply controlling the potential during the electrodeposition process. The growth mechanism is proposed by monitoring the morphology of the nanoparticles at different stages with scanning electron microscopy (SEM) and DFT calculations.

To obtain Ag nanoparticles, the electrode potential of the glassy carbon working electrode (GCE) was controlled at −0.7 V (vs. saturated calomel electrode, SCE) in a solution containing $AgClO_4$ (0.1 M), thiourea (0.9 M), NaCl (0.1 M), and $HClO_4$ (0.01 M). This potential was about 50 mV more negative than the peak potential for silver deposition in the cyclic voltammogram (CV; see the Supporting Information).

[a] Y.-M. Fang, Z.-B. Lin, Y.-M. Zeng, Prof. W.-K. Chen, Prof. G.-N. Chen, Prof. J.-J. Sun
Ministry of Education Key Laboratory of Analysis and Determination for Food Safety
College of Chemistry and Chemical Engineering
Department of Chemistry, Fuzhou University
Fuzhou, 350108 (China)
Fax: (+86) 591-22866135
E-mail: jjsun@fzu.edu.cn

[b] Prof. B. Ren, Prof. Z.-Q. Tian
State Key Laboratory of Physical Chemistry of Solid Surfaces and Department of Chemistry
College of Chemistry and Chemical Engineering
Xiamen University, Xiamen, 361005 (China)
Fax: (+86) 592-2186532
E-mail: bren@xmu.edu.cn

Supporting information for this article is available on the WWW under http://dx.doi.org/10.1002/chem.201000068.

The SEM image (Figure 1) of the electrodeposits reveals structures of spherical microparticles decorated with nanothorns. As can be seen from the SEM image, the diameter

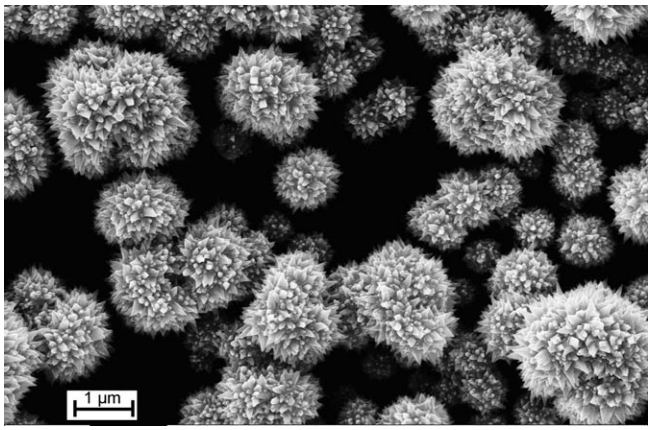

Figure 1. SEM image of Ag nanothorns electrodeposited at −0.7 V versus SCE for 60 s at a GCE. The solution contains $AgClO_4$ (0.1 M), thiourea (0.9 M), NaCl (0.1 M), and $HClO_4$ (0.01 M).

of the Ag microparticles is in the range of 0.5 to 2 μm and the nanothorn is in the range of 50 nm and radiates out from the microparticle cores. The TEM image of one of the electrodeposits also indicates the nanothorn structure (Figure 2A). The HRTEM (high-resolution transmission electron microscopy) images shown in Figure 2B and C (on a larger scale) reveal that the surface of nanothorn is oriented to the (111) plane, evidenced by the lattice spacing of 0.24 nm. This structure is very similar to the previous report of Pt nanothorns.[19]

To understand the growth mechanism of such nanothorns, we monitored the SEM images of the electrodeposits as a function of the deposition time. As clearly seen in Figure 3, at the beginning of deposition (Figure 3A, within 10 s), the electrodeposits are composed of silver particles with a large size distribution. The particles are formed by silver nanoparticles with a much smaller size, showing a spongelike appearance. With a prolonged deposition time (see Figure 3B–E), some protrusions appear on the particle surfaces and gradually grow into flakes with very sharp tips. Some small crystal nuclei begin to grow on the nanothorns after a long time deposition (Figure 3E). In electrochemistry, the nucleation mode of the electrodeposition process can be easily identified by the dimensionless plot of I^2/I_m^2 versus t/t_m (I = current, t = time; I_m and t_m are the maximum current and its corresponding time in the deposition process, respectively).[23] The nucleation process can be classified into instantaneous and progressive modes, which give the solid and dashed curves in Figure 4, respectively. By treating the experimentally obtained I/t curve in the above-mentioned way (for more details, see the Supporting Information) we obtained the dotted curve in Figure 4, which agrees well with the theoretical instantaneous nucleation mode. It indicates that the growth of Ag nanothorns goes through an instantaneous nucleation process, that is, the nanothorns grow from previously formed nuclei without the formation of new nuclei.

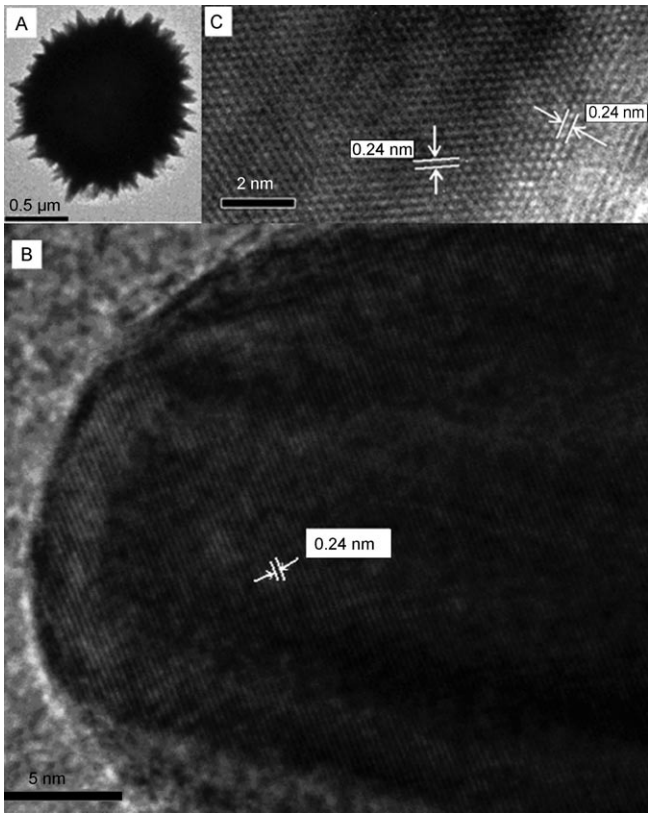

Figure 2. TEM image (A) and HRTEM images (B and C) of Ag nanothorns electrodeposited at −0.7 V versus SCE for 70 s at a GCE. The solution contains $AgClO_4$ (0.1 M), thiourea (0.9 M), NaCl (0.1 M), and $HClO_4$ (0.01 M).

We considered the influence of the composition of the solution further, that is, ClO_4^-, Cl^-, thiourea, and acidity, on the formation of Ag nanothorns. The SEM images of Ag deposited from different solutions are displayed in Figure 5. In the presence of thiourea, the nanothorn structures can be observed despite some minor differences in size and sharpness, indicating the similar growth mechanism in the presence of thiourea. Hence, thiourea is of vital importance for the formation of such a structure. In the absence of thiourea, the growth mechanism is unclear, and it is believed to be very different and somewhat complex because the dimensionless plot (I^2/I_m^2 vs. t/t_m) agrees with neither Figure 4A nor B. The CV and I/t curves are also very different from those with thiourea. The current is much larger, the peak potential is more positive, and the peak is somewhat ill-defined (for more details about the CV, the dimensionless plot, and I/t curves in different solutions, see the Supporting Information.) Combining the SEM images of the Ag morphologies monitored as a function of time in Figure 3, we believe that the instantaneous nucleation in the presence of thiourea is an important reason for the formation of Ag nanothorns. In the presence of thiourea, because of the for-

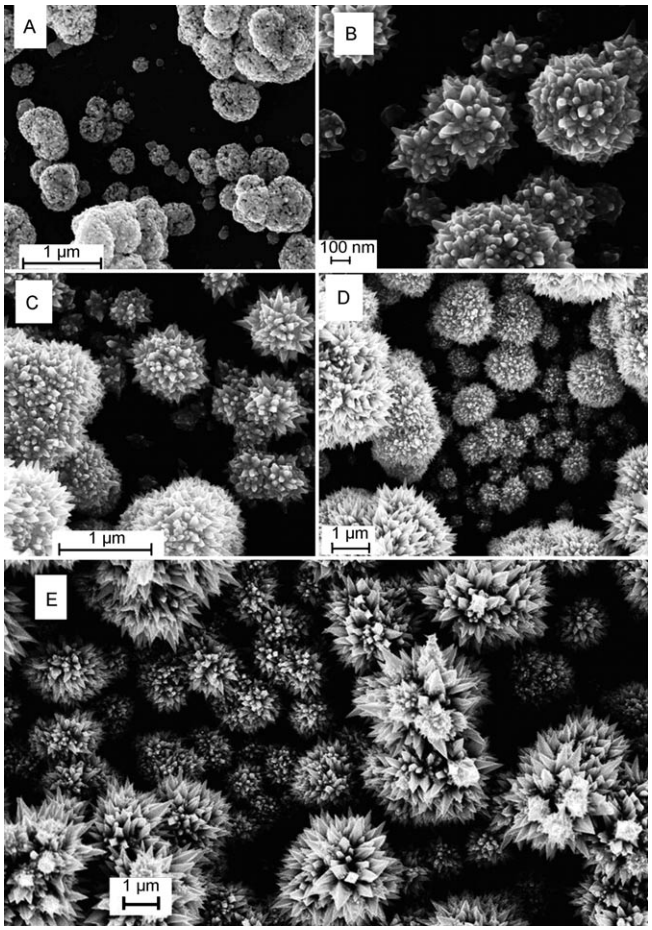

Figure 3. SEM images of Ag nanothorns electrodeposited at −0.7 V versus SCE for A) 10 s, B) 30 s, C) 60 s, D) 120 s, and E) 240 s at a GCE. The solution contains $AgClO_4$ (0.1 M), thiourea (0.9 M), NaCl (0.1 M), and $HClO_4$ (0.01 M).

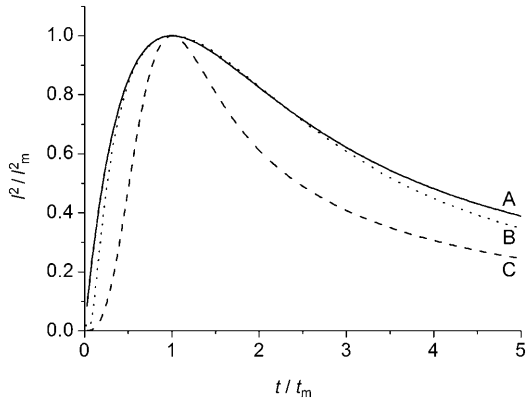

Figure 4. Dimensionless I^2/I_m^2 versus t/t_m plots for A) theoretical instantaneous nucleation (——), B) theoretical progressive nucleation (-----), and C) the experimental results (•••••).

mation of stable Ag–thiourea complexes, the reduction of Ag^+ is significantly inhibited as the onset deposition potential shifts by approximately −800 mV compared with the potential in the absence of thiourea. The formation of Ag

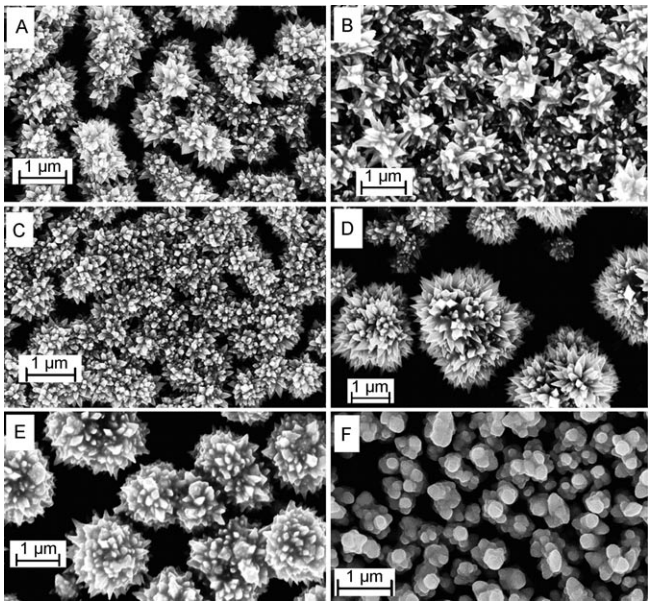

Figure 5. SEM images of Ag nanothorns electrodeposited at A) $AgClO_4$ (0.1 M), thiourea (0.9 M), and NaCl (0.1 M); B) $AgClO_4$ (0.1 M), thiourea (0.9 M), and $HClO_4$ (0.01 M); C) $AgClO_4$ (0.1 M), thiourea (0.9 M), NaCl (0.1 M), and $HClO_4$ (0.01 M); D) $AgClO_4$ (0.1 M), thiourea (0.9 M), NaCl (0.1 M), and $HClO_4$ (0.1 M); E) $AgClO_4$ (0.1 M), thiourea (0.9 M), NaCl (0.1 M), and HCl (0.01 M); and F) $AgClO_4$ (0.1 M), and $HClO_4$ (0.01 M) for 60 s.

nuclei is a very unfavorable process at the GCE, as evidenced by the negative shift of the onset deposition potential of approximately 250 mV compared with that on the Ag electrode (for more details, see the Supporting Information). When a much more negative potential is applied, approximately −50 mV more negative than the peak potential, the Ag nuclei are forced to generate (the birth of a new phase of Ag particles). Because the formation of Ag nuclei is a very unfavorable process, no more Ag nuclei are generated in the presence of thiourea, thus, the growth of Ag particles follows the instantaneous mode rather than the progressive mode. Owing to the high surface area to volume ratio of Ag nuclei, the Ag nuclei group together as shown in Figure 3A and act as seeds for the growth of Ag nanothorns.

As demonstrated in Figure 5, thiourea plays an important role in the formation of the nanothorn structures. Recalling the (111) crystal structure of the nanothorn, we may propose two possible reasons: 1) Thiourea prefers to be adsorbed on the Ag (111) plane than others such as the Ag (100) or Ag (110), resulting in a lower growth rate in the (111) direction and a final structure with the Ag (111) plane being dominant; 2) The relatively low surface energy of the Ag (111) plane leads to that fact that the growth on this plane is not favorable. To clarify these reasons, we performed DFT calculations[24,25] of the adsorption energy of thiourea and the surface energy of different crystal facets (for more details, see the Supporting Information). As indicated in Table 1, the adsorption energy of thiourea on the Ag (111) plane is not higher than those of the other planes, whereas its surface energy is the lowest. Therefore, we pro-

Table 1. Adsorption energy of thiourea and the surface energy at different crystal faces of Ag calculated by DFT methods.

	Ag (111)	Ag (100)	Ag(110)
surface energy[a]	0.8088	1.1134	0.9841
adsorption energy[b]	−90.37	−90.78	−93.98

[a] The unit of surface energy is $J m^{-2}$; [b] The unit of adsorption energy of thiourea at the Ag surface is $kJ mol^{-1}$. For more calculation details, see the Supporting Information.

pose that the high predominant orientation of the Ag (111) plane could be attributed to the lower surface energy of the plane. In the presence of thiourea, the formation of stable Ag–thiourea coordination complexes, as well as the adsorption of thiourea on the Ag surface, could inhibit the surface reaction leading to a decrease of the current density and growth rate (see the Supporting Information), which facilitates the growth of the well-defined Ag (111) plane.

The unique nanothorn structure makes it a very unique substrate for SERS. The SERS experiment was performed with thiourea as the probe molecule. The SERS spectra presented in Figure 6 shows the unique feature of thiourea on

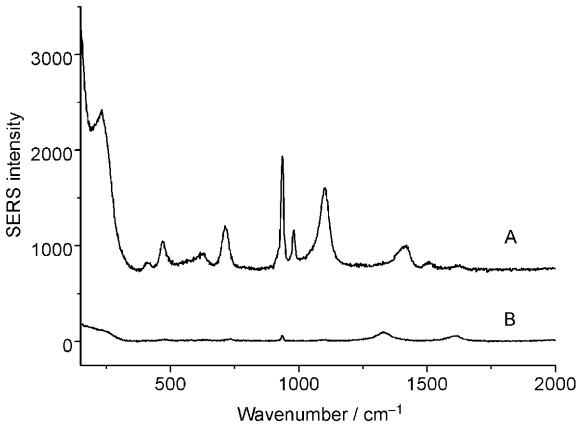

Figure 6. SERS activity of thiourea in thiourea (0.1 M) and $HClO_4$ (0.01 M) at A) Ag nanothorns electrodeposited in $AgClO_4$ (0.1 M), thiourea (0.9 M), and NaCl (0.1 M) for 100 s; B) Ag nanopaticles deposited in $AgClO_4$ (0.1 M) and $HClO_4$ (0.01 M) for 100 s.

Ag electrode (the broad feature in the region of 1300 to 1600 cm^{-1} in Figure 6B is from the GCE substrate).[26,27] The SERS activity of Ag nanothorns of the sample in Figure 5A is about 20 folds stronger than that of the Ag nanopaticles without the thorn structure (see Figure 5F). We also investigated other probe molecules such as thiocyanate (SCN^-) and a similar trend was obtained, indicating that nanothorns can be used as good SERS substrates.

We have proposed a facile method for the preparation of Ag nanothorns with good SERS activity. The Ag nuclei are instantaneously generated and gradually grow into nanothorn structures. The (111) surface is predominant because it has the lowest surface energy. The Ag nanothorns may have applications in fields such as SERS and sensing.

Experimental Section

The electrochemical experiments were carried out on a CHI 604b electrochemical analyzer (Chenhua Instruments, Shanghai, China) in a traditional three-electrode cell. A GCE, 3 mm in diameter, was used as the working electrode, a SCE and a Pt foil were used as the reference and counter electrodes, respectively. Deionized water with a resistivity of 18.2 MΩ cm (Millipore, Bedford, MA, USA) was used throughout the experiments. The calculations were carried out by using the Dmol^3 program package of Materials Studio (Accelrys) based on DFT calculations. The TEM and HRTEM study was performed on a TECNAI F-30 high-resolution transmission electron microscope operating at 300 kV. The SEM study was performed on a LEO1530 scanning electron microscope with a field emission electron gun operated at 20 kV. The SERS measurement was performed on a LabRam I confocal microscope Raman system (Horiba/JY, France) at 632.8 nm excitation from an air-cooled He–Ne laser.

Acknowledgements

The authors thank the National Science Foundation of China (Nos. 20775015, 20735002, and 20975022), National Basic Research Program of China (No. 2010CB732403), Specialized Research Fund for Doctoral Program of Higher Education (20070386005) from MOE, the program for NCETTFJ (XSRC2007-02), and the open funding of the State Key Laboratory of Physical Chemistry of Solid Surfaces of Xiamen University for financial support.

Keywords: crystal growth · electrochemistry · nanostructures · Raman spectroscopy · silver

[1] Y. Xia, Y. Xiong, B. Lim, S. E. Skrabalak, *Angew. Chem.* **2009**, *121*, 62; *Angew. Chem. Int. Ed.* **2009**, *48*, 60.
[2] B. Wiley, Y. Sun, Y. Xia, *Acc. Chem. Res.* **2007**, *40*, 1067.
[3] B. Wiley, Y. Sun, B. Mayers, Y. Xia, *Chem. Eur. J.* **2005**, *11*, 454.
[4] Y. Sun, Y. Xia, *Science* **2002**, *298*, 2176.
[5] A. Tao, P. Sinsermsuksakul, P. Yang, *Angew. Chem.* **2006**, *118*, 4713; *Angew. Chem. Int. Ed.* **2006**, *45*, 4597.
[6] B. Wiley, T. herricks, Y. Sun, Y. Xia, *Nano Lett.* **2004**, *4*, 1733.
[7] X. Sun, S. Dong, E. Wang, *Angew. Chem.* **2004**, *116*, 6520; *Angew. Chem. Int. Ed.* **2004**, *43*, 6360.
[8] B. Liu, J. Xie, J. Y. Lee, Y. P. Ting, J. P. Chen, *J. Phys. Chem. B* **2005**, *109*, 15256.
[9] S. Guo, S. Dong, E. Wang, *Cryst. Growth Des.* **2009**, *9*, 372.
[10] B. J. Wiley, Y. Xiong, Z. Y. Li, Y. Yin, Y. Xia, *Nano Lett.* **2006**, *6*, 765.
[11] R. Narayanan, M. A. EI-Sayed, *Nano Lett.* **2004**, *4*, 1343.
[12] M. Bode, O. Pietzsch, A. Kubetzka, R. Wiesendanger, *Phys. Rev. Lett.* **2004**, *92*, 067201.
[13] Z. B. Lin, J. H. Tian, B. G. Xie, Y. A. Tang, J. J. Sun, G. N. Chen, B. Ren, B. W. Mao, Z. Q. Tian, *J. Phys. Chem. C* **2009**, *113*, 9224.
[14] Y. W. C. Cao, R. C. Jin, C. A. Mirkin, *Science* **2002**, *297*, 1536.
[15] C. L. Haynes, A. D. McFarland, R. P. Van Vuyne, *Anal. Chem.* **2005**, *77*, 338A.
[16] S. Nie, S. R. Emory, *Science* **1997**, *275*, 1102.
[17] K. L. Kelly, E. Coronado, L. L. Zhao, G. C. Schatz, *J. Phys. Chem. A* **2003**, *107*, 668.
[18] P. F. Liao, A. Wokaun, *J. Chem. Phys.* **1982**, *76*, 751.
[19] N. Tian, Z. Y. Zhou, S. G. Sun, L. Cui, B. Ren, Z. Q. Tian, *Chem. Commun.* **2006**, 4090.
[20] P. He, H. Liu, Z. Li, Y. Liu, X. Xu, J. Li, *Langmuir* **2004**, *20*, 10260.
[21] N. Tian, Z. Y. Zhou, S. G. Sun, Y. Ding, Z. L. Wang, *Science* **2007**, *316*, 732.

[22] Z. Y. Zhou, N. Tian, Z. Z. Huang, D. J. Chen, S. G. Sun, *Faraday Discuss.* **2009**, *140*, 81.
[23] B. Scharifker, G. Hills, *Electrochim. Acta* **1983**, *28*, 879.
[24] B. Delley, *J. Chem. Phys.* **1990**, *92*, 508.
[25] B. Delley, *J. Chem. Phys.* **2000**, *113*, 7756.
[26] T. Ishiguro, E. Suzuki, A. Y. Hirakawa, M. Tsuboi, *J. Mol. Spectrosc.* **1980**, *83*, 360.
[27] Z. Q. Tian, Y. Z. Lian, M. Fleischmann, *Electrochim. Acta* **1990**, *35*, 879.

Received: January 12, 2010
Published online: May 10, 2010

